

Nanoreservoir Operated by Ferrocenyl Linker

Oxidation with Molecular Oxygen

Gleiciani Q. Silveira, Maria D. Vargas,* and Célia M. Ronconi*

Instituto de Química, Universidade Federal Fluminense, Outeiro de São João Batista, s/n, Campus do Valongo, Centro, 24.020-141, Niterói, RJ, Brazil

E-mail: mdvargas@vm.uff.br; cmronconi@vm.uff.br

Supporting Information

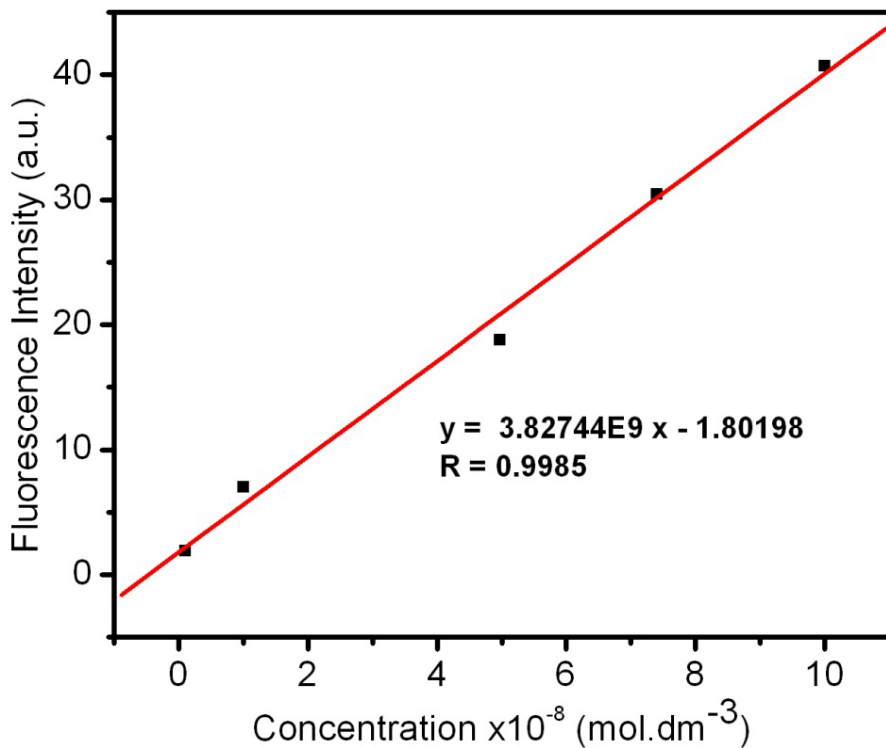


Figure S1. Standard addition curve of rhodamine B used to estimate the loading efficiency of rhodamine B into the FcMCM-41 pores and the amount of dye released from the nanoreservoir into the solution. In the first experiment, the washings were combined for the determination of the concentration of rhodamine B and the amount of loaded rhodamine B was determined by difference from the initial concentration.

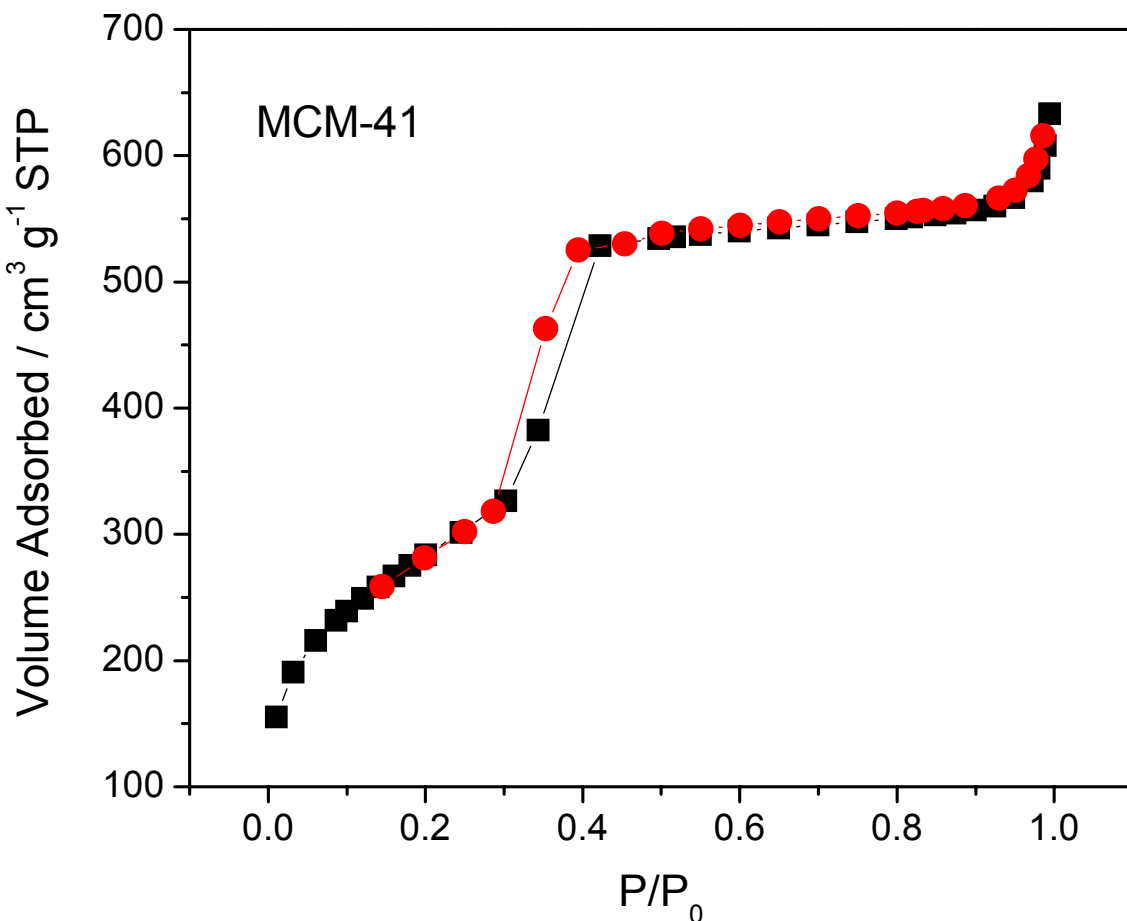


Figure S2. Nitrogen adsorption/desorption isotherms of the MCM-41.

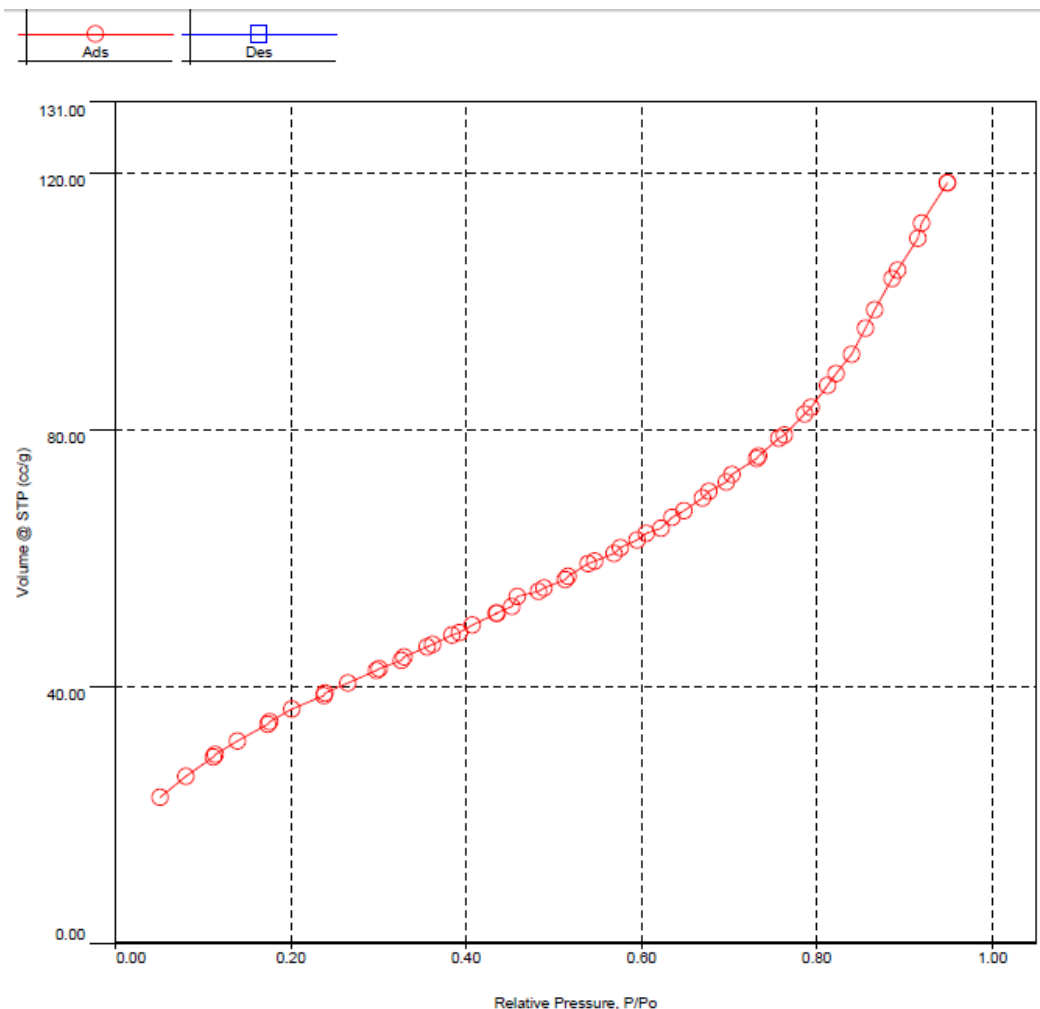


Figure S3. Nitrogen adsorption isotherms of the APMCM-41.

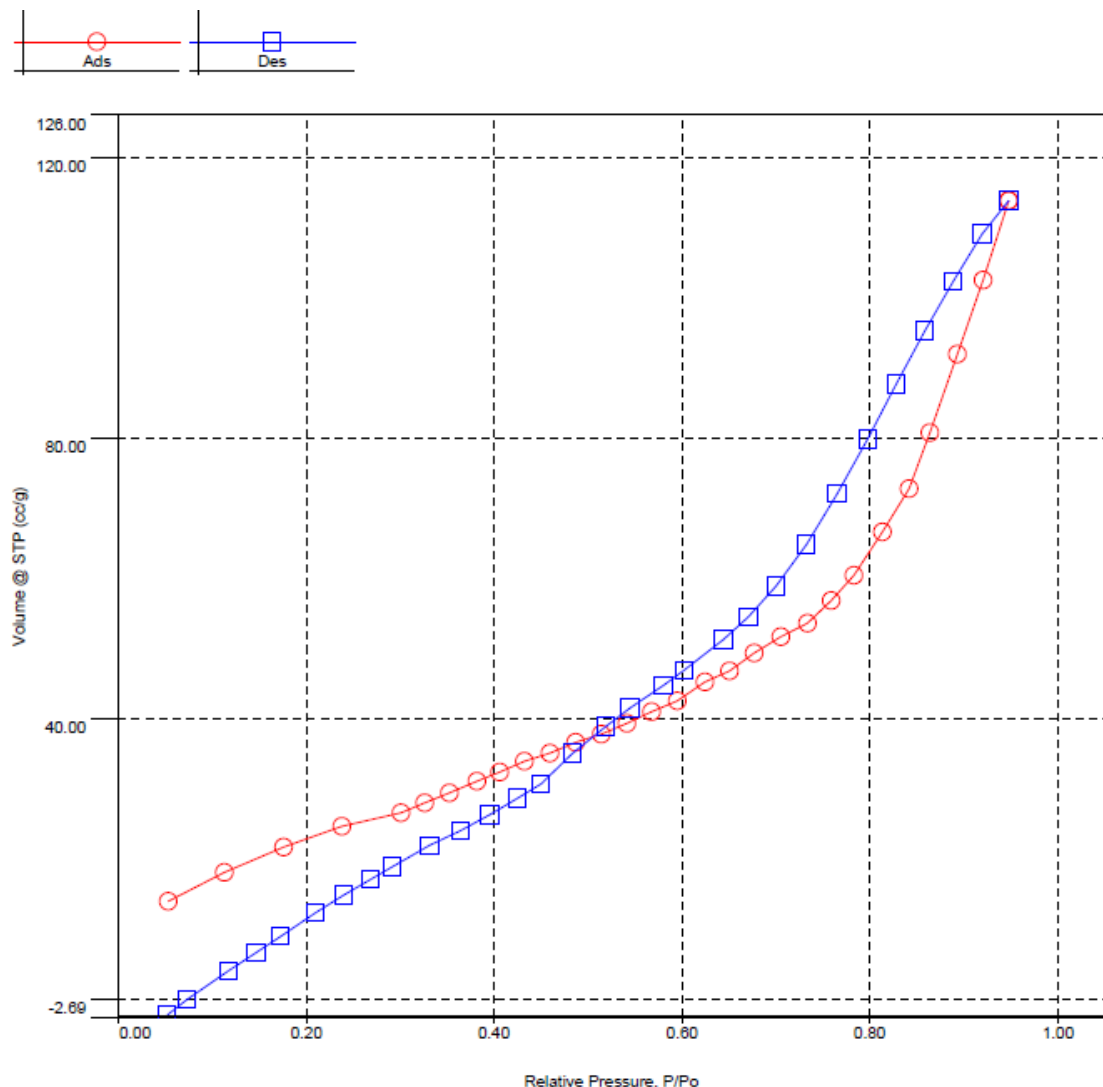


Figure S4. Nitrogen adsorption/desorption isotherms of the FcMCM-41.

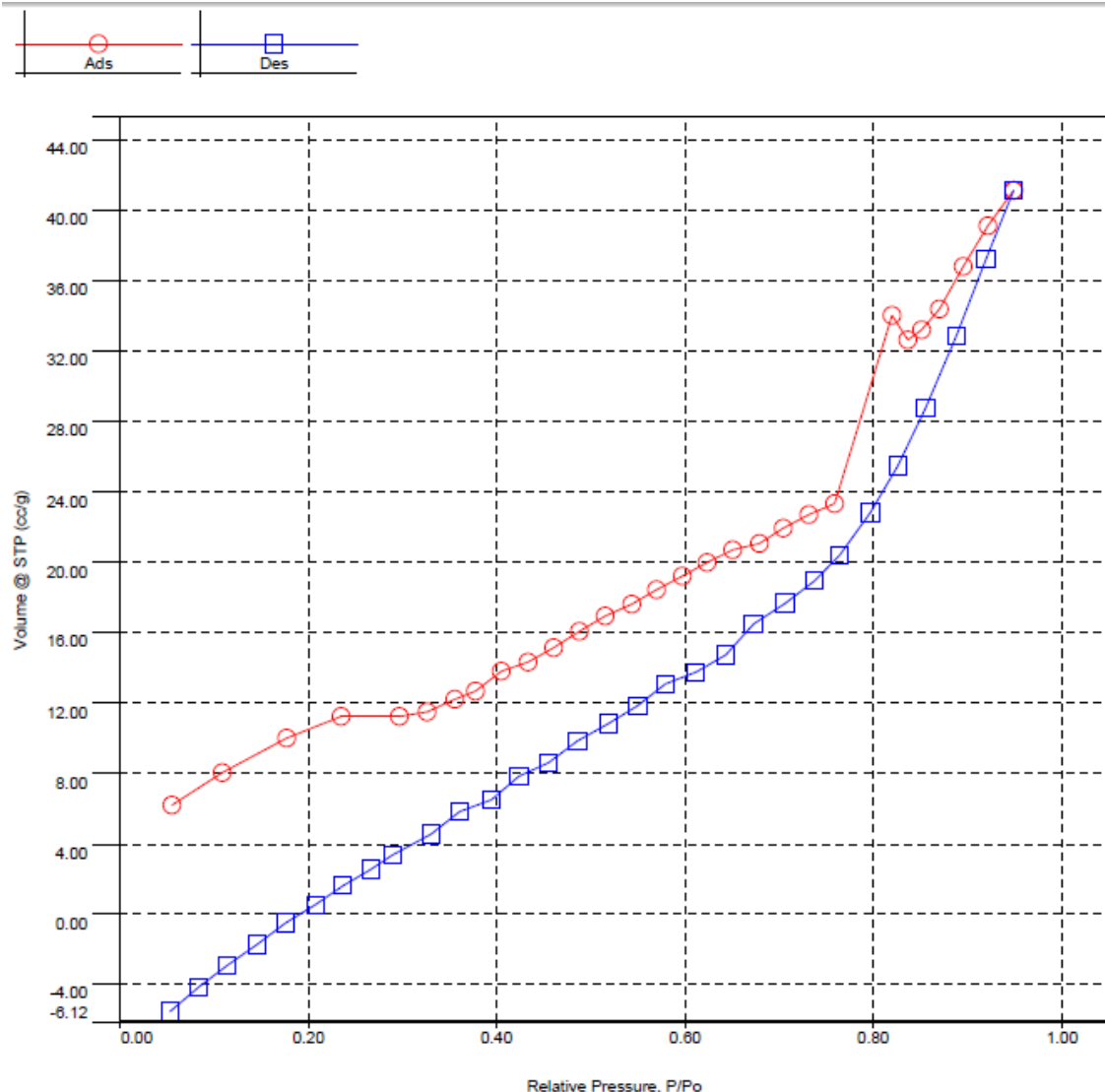


Figure S5. Nitrogen adsorption/desorption isotherms of the rhodamine B-loaded FcMCM-41- β -CD.

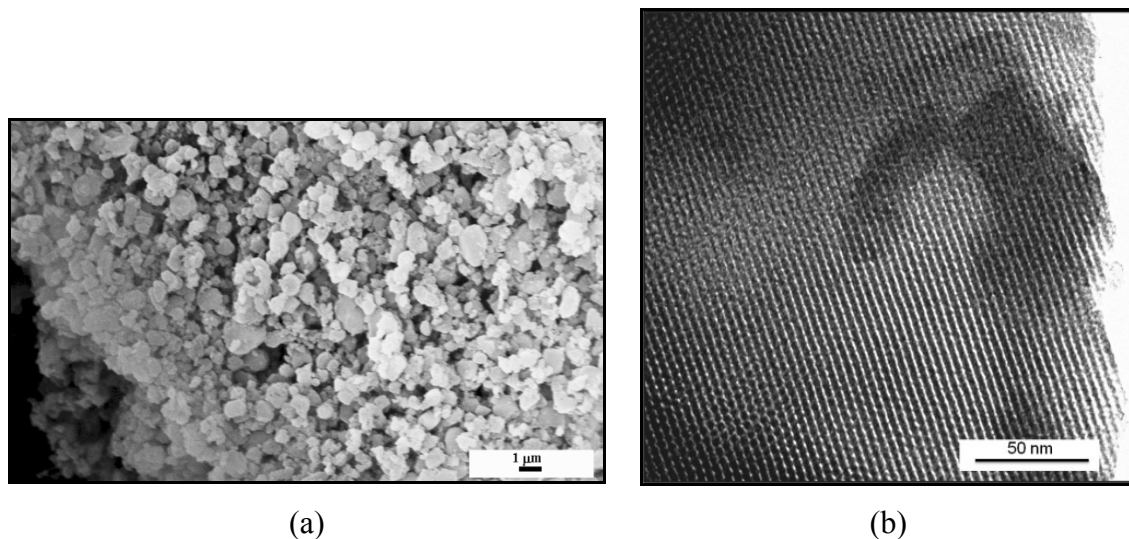


Figure S6. (a) Scanning electron (SEM) and (b) transmission electron micrographs (TEM) of MCM-41.

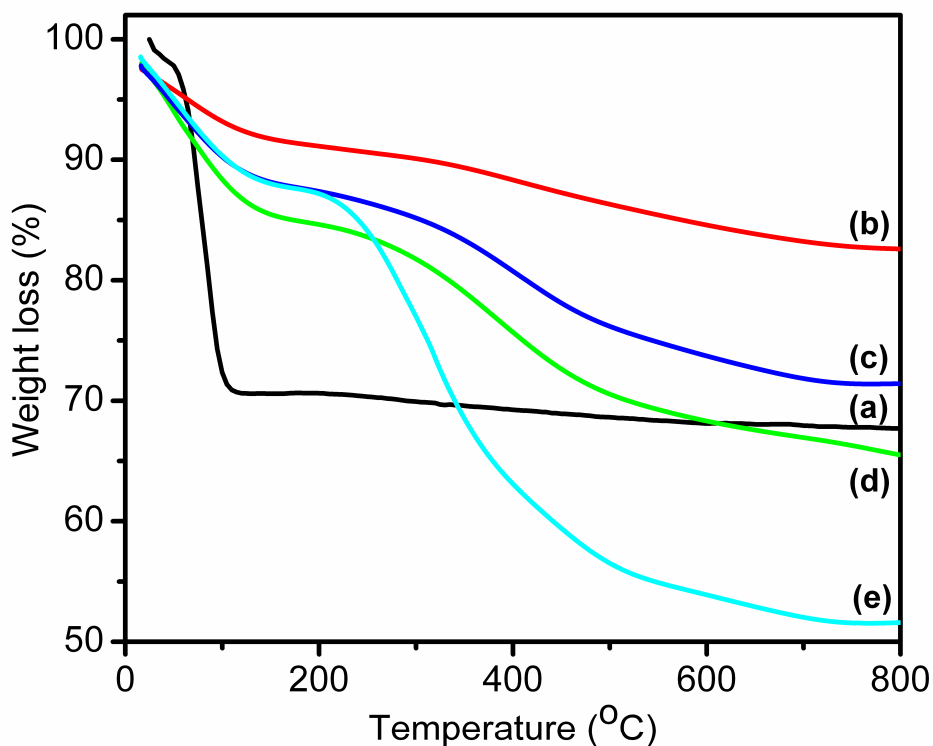


Figure S7. TGA curves of (a) MCM-41, (b) APMCM-41, (c) FcMCM-41, (d) rhodamine B-loaded FcMCM-41 and (e) rhodamine B-loaded FcMCM-41 \subset β -CD.

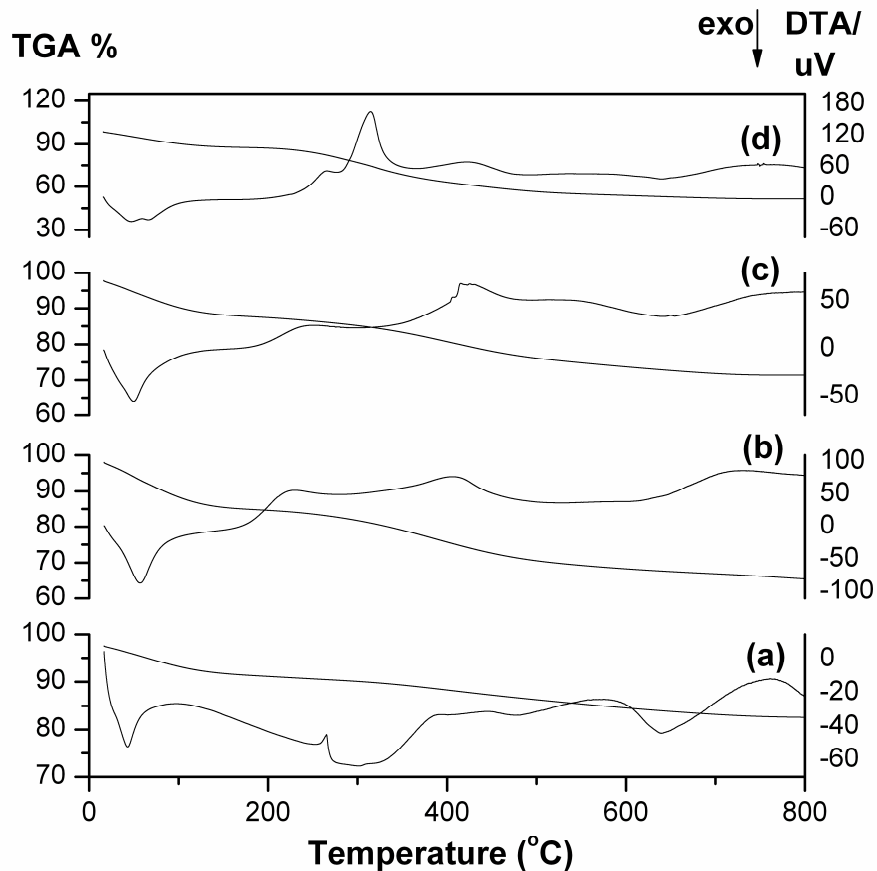


Figure S8. DTA-TG curves of (a) APMCM-41, (b) FcMCM-41, (c) rhodamine B-loaded FcMCM-41 and (d) rhodamine B-loaded FcMCM-41 $\subset\beta\text{-CD}$.

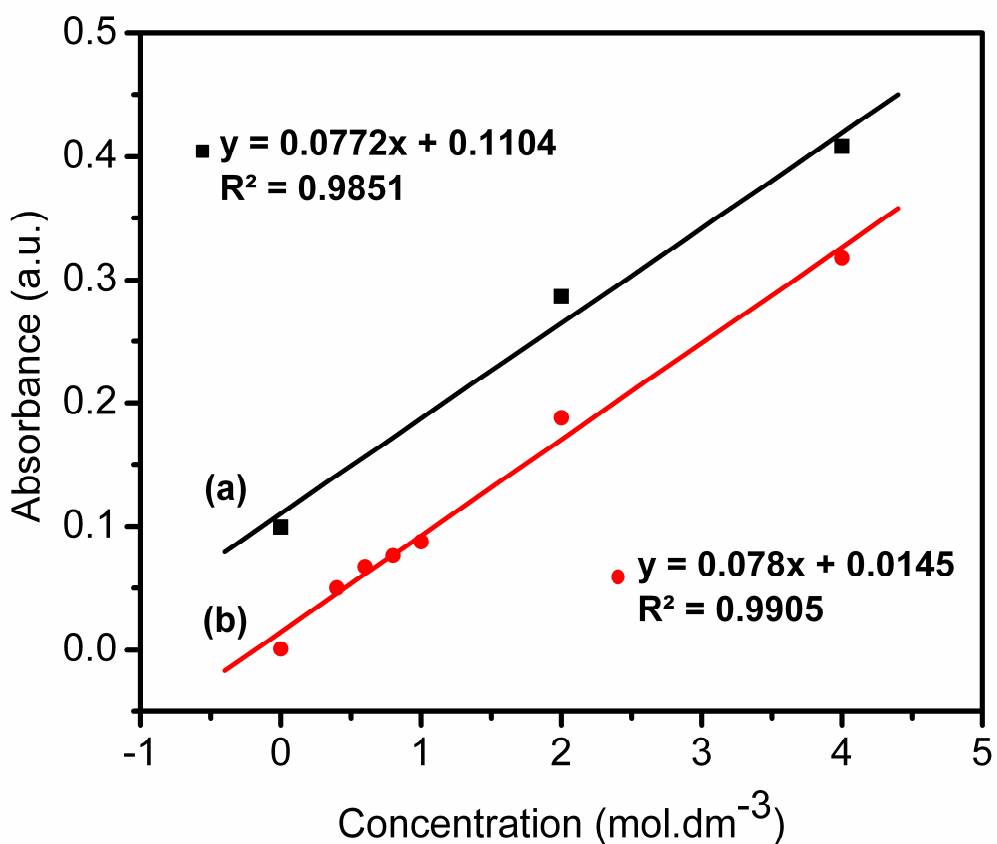


Figure S9. Atomic absorption of iron: (a) analytic curve and (b) standard addition curve.

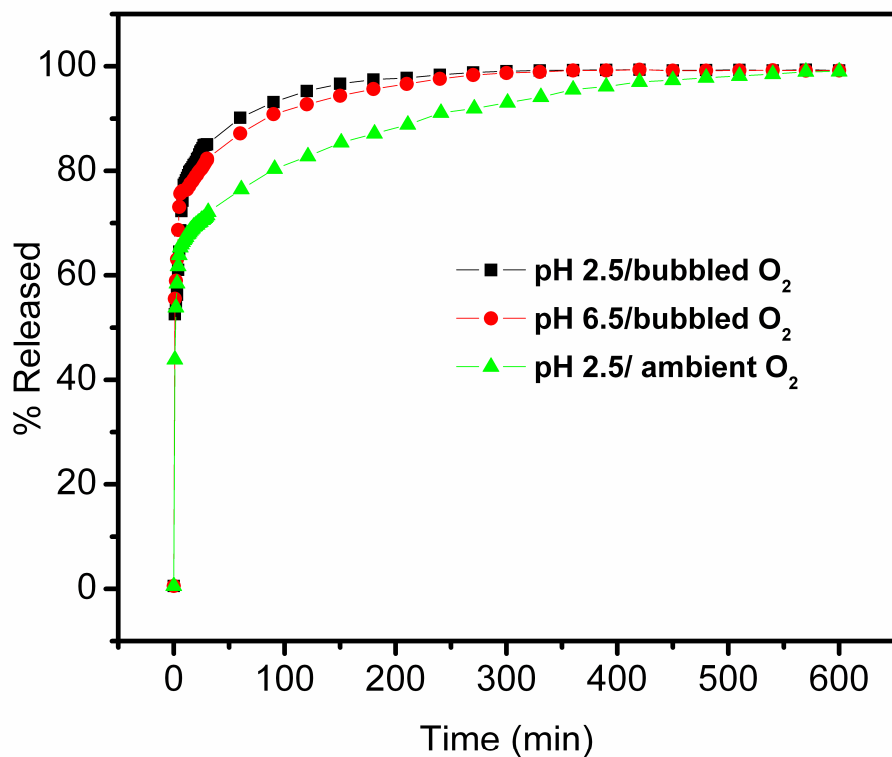


Figure S10. Release profiles of rhodamine B from the nanoreservoir in aqueous solution at different pH values as a function of time.

